Received 25 June 2023; revised 23 August 2023 and 7 September 2023; accepted 14 September 2023.
Date of publication 20 September 2023; date of current version 9 October 2023.

Digital Object Identifier 10.1109/OJUFFC.2023.3317363

Graded Elastic Waveguide Metamaterial Rod for Up-Conversion of Longitudinal Axisymmetric Guided Ultrasonic Wave Modes

S. R. SANDEEP KUMAR[1], VINEETH P. RAMACHANDRAN[1,2], KRISHNAN BALASUBRAMANIAM[1], AND PRABHU RAJAGOPAL[1]

[1]Centre for Nondestructive Evaluation and Department of Mechanical Engineering, Indian Institute of Technology Madras, Chennai, Tamil Nadu 600036, India
[2]DRDO Young Scientists' Laboratory for Smart Materials, Hyderabad 500058, India

CORRESPONDING AUTHOR: S. R. SANDEEP KUMAR (sandeepkumariitm@gmail.com)

The work of Prabhu Rajagopal was supported in part by the National Swarnajayanti Fellowship Award.

ABSTRACT Cylindrical or circular rod-type waveguides are of much interest in applications such as measurement of flow, temperature, material properties in harsh environments, and also in medical diagnostics. However, multiple waveguide modes exist in such systems, out of which only some are of interest to certain applications. For example, L(0,3) longitudinal mode excitation can optimally transmit elastic waves into the test specimen and help in better sensing and measurement when compared to other modes within the family of longitudinal guided waves. This paper demonstrates the up-conversion of longitudinal modes within the family of guided ultrasonic rod waves (from L(0,2) to L(0,3)), which is of interest to certain waveguide transducer applications. The mode up-conversion is demonstrated using numerical simulations and experiments. An analysis is used to bring more insights and guide the design of the metamaterial in this process.

INDEX TERMS Metamaterials, periodic structures, rods, mode filter, guided waves, longitudinal modes, graded elastic metamaterial rods, ultrasonic waveguides.

I. INTRODUCTION

WAVEGUIDES are extended structures used for confining and guiding elastic and other types of waves, initially studied widely in the context of measurement of flow [1], [2]. Today they find applications in the remote monitoring of temperature [3], viscosity [4], [5], environmental parameters [6], material properties [7], [8], setting of concrete [9], [10], [11] and curing of composites [12], especially when the vulnerable transducers and piezoelectric elements need to be isolated from harsh environments. Examples are the measurement of thickness at temperatures >500°C [13], thickness of hot plates and molten metals up to 960°C and online monitoring of polymer extrusion [14]. Another example is the development of distributed temperature sensor for measurement of temperatures of the order 900°C from multilocations as many as 18, using a single wire waveguide [15], [16]. The underlying physics in those methods is; waveguide sensors measure changes in time of flight of a guided ultrasonic wave mode caused due to the changes in the material properties of the waveguide as a function of temperature. Ultrasonic guided waves are elastic waves propagating in extended structures such as plates, pipes and rods [17], [18], [19], [20]. Guided waves are attractive for rapid inspection of infrastructural assets such as pipelines, pavements and storage tanks. This is primarily because fundamental guided waves can propagate long distances from a single location and also have a through-thickness signature. However, each guided wave family consists of multiple modes differing in their sensitivity towards the position and nature of the defect. It is, therefore, a challenging task in ultrasonics to filter out such additional modes.

In the case of cylindrical rods used as waveguides for guided ultrasonic wave propagations, multiple modes such as families of torsional, longitudinal, and flexural modes

exist. To overcome this difficulty, researchers typically (see, for example, Sandeep et al. [21]) proposed filtering out certain modes from the above with the help of metamaterials and using the most suitable one for specific applications. Metamaterials are artificially engineered materials displaying exotic behaviour not found in nature. Over the last two decades many applications of novel metamaterials have been demonstrated, but not limited to, i.e., focusing/ controlling of waves [22], [23], subwavelength resolution imaging [24], [25], [26], sensing [27], cloaking [28], [29], negative refraction [30], [31], negative Poisson's ratio [32], [33], [34], [35], seismic wave protection [36], vibration and sound suppression [37], [38], [39], [40] etc. Another interesting feature of metamaterials is their ability to create bandgaps, i.e.; frequency bands within which the propagation of elastic wave is prohibited. There are mainly two types of bandgaps, viz; Bragg and locally resonant bandgaps. The destructive interference of two waves induced by the periodicity of unit cells of the order of wavelength is the main mechanism of Bragg bandgap, whereas, the mechanical resonance of scatterers embedded inside a host matrix at wavelengths of orders much longer than the lattice constant of a unit cell is the mechanism of the locally resonant bandgap.

Graded metamaterial structures are typically used for energy localisation and energy harvesting purposes. De Ponti et al. [41], [42] investigated both numerically and experimentally of the surface elastic Rayleigh wave trapping in a graded metamaterial and its application in real energy harvesting performances. The graded array of resonating rods is employed to manipulate the wave propagation, by means of wavenumber transformation along the structure. On one hand, the waves are slowed-down and the interaction time between the wave and the harvester is increased, which is the blueprint of the *rainbow effect*. On the other hand, the wavenumber transformation is accompanied by a strong amplification inside the rods. Leveraging the interplay of these two effects, they illustrated that, the mechanical delay line is able to harvest six times the energy of a single harvester when compared to the normal case. Jo et al. [43] proposed a graded structure, by varying the height of the circular stub, with double defects for broadband energy localization and harvesting purposes. This method leads to localizing elastic waves in the vicinity of each defect at the designed different defect band frequencies and harvesting of energy.

In another study De Ponti et al. [44] experimentally achieved wave-mode conversion and rainbow trapping in an elastic waveguide loaded with a graded array of resonators with variable length. By breaking the geometrical symmetry of the waveguide with respect to the shear center of the waveguide, the impinging flexural waves are mode converted to torsional waves traveling in the opposite direction. Most studies reported so far focused on the conversion from one family of modes to another (longitudinal to transverse [45], Lamb to shear waves [46], [47], flexural to torsional [48] etc.) in plate-like structures. More recently, Colombi et al. [49] demonstrated how forests could act as a seismic metamaterial offering protection from earthquakes. Researchers from the same group later demonstrated experimentally the conversion and enhancement of Rayleigh waves into bulk shear waves by using metasurfaces in the ultrasonic regime [50]. Tian et al. demonstrated *'rainbow trapping'* of guided ultrasonic waves in chirped phononic crystal plates, whereby guided wave energy gets concentrated at different axial locations at different frequencies [51]. Recently, the author's group experimentally demonstrated deep subwavelength ultrasonic imaging using holey-structured metamaterial lenses [52], [53], wavefront manipulation using metamaterial [54] plates, focusing of ultrasound using 'material contrast' lenses [55] and frequency filtering [56], [57]. The mode conversion within the same family of modes in plate-like structures was also demonstrated. For example, Bavencoffe et al. [58] showed the coupling between two Lamb wave modes and an energy transfer from the incident mode to the converted mode in a plate with a periodic grating. However, to the best of our knowledge, there are very few reports on mode conversion within a given family of guided ultrasonic wave modes in rod-like structures, a phenomenon that is of much interest for waveguide transducer development [59]. This paper discusses a metamaterial technique (called a 'graded metamaterial rod' or GMR) for 'up-conversion' within the family of axisymmetric longitudinal rod-guided ultrasonic wave modes, L(0,n), which was impossible using conventional waveguides.

The advantage of such selective excitation of certain guided wave or waveguide modes is a major requirement in many non-destructive evaluation (NDE) applications, as discussed, for example, in a recent research article see [59] by the authors, for the generation of longitudinal bulk ultrasonic waves inside a sample using waveguide transduction. In that study, longitudinal guided waves, L(0,n), $n = 1,2,3,4$, were excited using magnetostrictive strips in a cylindrical waveguide for measurement of temperature in a rectangular block. It was proven both numerically and experimentally that the transmission ratio (ratio of amplitude of transmitted bulk ultrasonic waves into the specimen to the amplitude of excitation wave) is highest for L(0,3) compared to other modes. This high transmission ratio was attributed to the symmetric and unidirectional (positive) nature of L(0,3) wave mode across the cross-section of the waveguide. They also studied the quality of the signal transmitted to the specimen for all modes. Signal to noise ratios (SNR) in dB, obtained experimentally from ratios of the signal reflected from the free rear end of the test specimen to an averaged value of the noise signal from the A-scans for each of the excitation modes, showed the best for L(0,3) as against others.

However, using patch transduction for such applications (as was done in [59]) has its own drawbacks, including the necessity for special types of excitation such as magnetostriction. Here, we propose a metamaterial-based a 'mechanical filter' approach, as illustrated in Fig. 1 below, to selectively enhance the L(0,3) mode in circular rod waveguides.

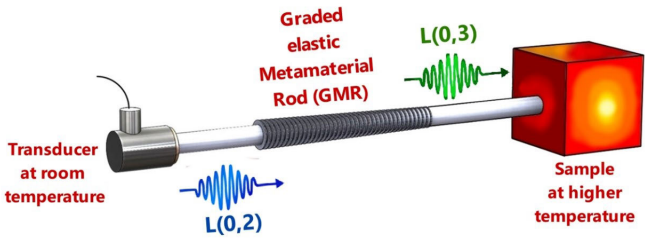

FIGURE 1. Schematic showing the possible application of the proposed GMR, enabling the up-conversion of L(0,2) longitudinal wave mode to L(0,3) longitudinal wave mode for enhanced sensing of high temperature sample.

To the best of the authors' knowledge, the main contributions of this study include:

1) Earlier works of researchers focused on mode conversion from one family of modes to another (longitudinal to transverse, Lamb to shear waves, flexural to torsional etc.), but not within the same family of modes, in plate-like structures.

2) This paper demonstrates the up-conversion of longitudinal modes within the family of guided ultrasonic rod waves (from L(0,2) to L(0,3)), which is of interest to certain waveguide transducer applications.

This article is organized as follows. Firstly, a numerical simulation of longitudinal elastic wave propagation in a GMR showing the mode conversion is discussed, followed by the presentation of experimental validation results. An analysis is then used to bring more insight into the process. The paper concludes with directions for future work.

II. METHODS

A. PROBLEM STUDIED

We consider a 10mm diameter Aluminium cylindrical rod waveguide of 1m length. In this waveguide, the possible guided ultrasonic wave modes are obtained by using DISPERSE software [60], as shown in Fig. 2. It should be noted that DISPERSE is used for generating dispersion curves of guided wave modes in uniform cylindrical waveguides (waveguides of constant diameter throughout the length).

We can observe from Fig. 2 that multiple modes exist at the operating frequency of 0.5 MHz. The aim of the present work is to convert some of these modes to other mode within the family of waves using the proposed GMR of inner diameter 10mm as shown in Fig. 3. This design is inspired by the use of similar concepts with varying 'baffle' heights as proposed in the context of flat or plate-like structures in literature [48]. In Fig. 3, $t = 0.5$mm and $L = 2.5$mm throughout the waveguide, and the value of annular ring (or 'baffle' henceforth) width (H) is varied from 2.5mm to 0.5mm spanning 40 Nos of baffles in the direction of wave propagation. Since elastic wave velocity is dependent on the diameter of circular rods, repeated variation of the cross-sectional area will induce a change in wave propagation velocity. Similar phenomenon was earlier used for mode conversion in the plate-type waveguides [49], [50]. Inspired by this

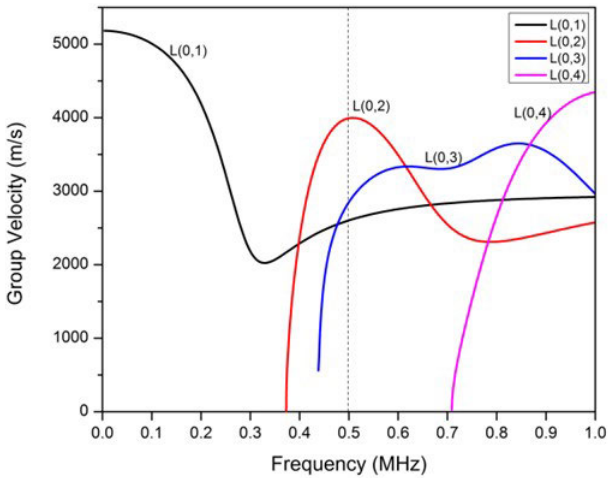

FIGURE 2. Group velocity dispersion curves generated using DISPERSE [60] software for a ϕ10 mm aluminium cylindrical rod indicating different guided wave modes of interest.

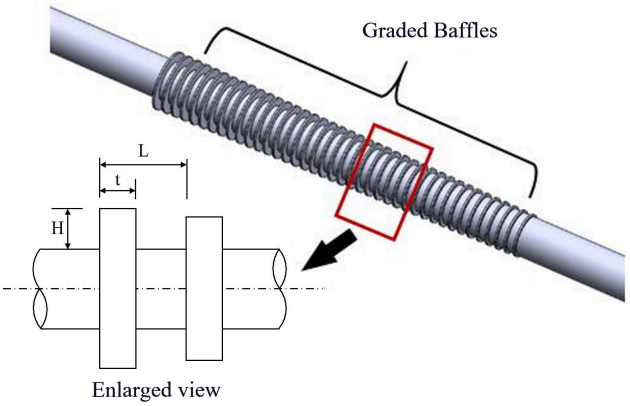

FIGURE 3. 3D CAD model of the proposed GMR concept, showing geometric parameters in the inset.

idea of using graded metasurfaces, 3D Finite Element (FE) simulations were performed for various cases and arrived at the above dimension. As already mentioned above, generating dispersion curves for such non-uniform waveguides cannot be done using DISPERSE. For each of the baffle of finite length and fixed diameter in our GMR, we have used DISPERSE for generating the dispersion curve and finally used an approach via group delay calculation for arriving at the dispersion relation for the whole GMR. These results, presented in Section III-B below, support the 3D FE results.

B. NUMERICAL SIMULATION

In order to understand the wave propagation in the GMR, a three-dimensional explicit time FE model was created in a commercial package [61]. The model was meshed using 4-node bilinear axisymmetric quadrilateral elements (CAX4R) with a size of 0.1 mm. An excitation was given in the form of nodal forces as a Hanning windowed tone-burst with central frequency at 0.5 MHz, and the displacements were monitored at the other end of the rod. Here we focus on a mid-frequency of 0.5 MHz since this is of much interest to

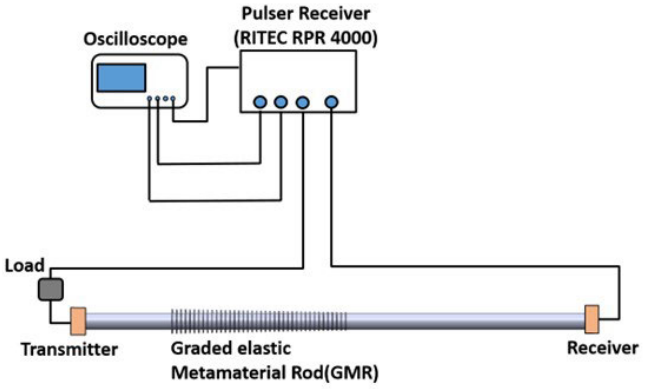

FIGURE 4. Schematic of the Experimental Setup used to demonstrate the up-conversion of L(0,2) to L(0,3) modes.

the development of waveguide ultrasonic sensors [59]. The model was computed for a total time of 400 μs with a step time increment of 1ns. The time traces (A-scans) obtained from these simulations were further analysed by obtaining the frequency spectrum, as discussed below in Section III-A.

C. EXPERIMENTS

Guided ultrasonic wave experiments with the circular rod-guided, ultrasonic wave mode L(0,2) were conducted on a sample with the proposed waveguide concept with the goal of converting this mode to useful L(0,3) mode at the target frequency 0.5 MHz. The GMR is made of Aluminium with surface baffles manufactured by turning operation in Computer Numerical Control (CNC) machine.

The experimental set-up shown in Fig. 4 consists of two contact transducers (V101-0.5MHz Panametrics Inc., Waltham, MA, USA), located at either end of the rod waveguide acting as the transmitter and receiver, respectively. Guided ultrasonic waves of the longitudinal family were generated using a commercially available transducer of a central frequency of 0.5 MHz. A 10-cycle toneburst Hanning windowed pulse was generated by the pulser-receiver (RPR-4000 RITEC Inc., Warwick, Rhode Island, USA) in the pitch-catch configuration. The signals obtained from the transducer connected at the receiving end were displayed and recorded using a digital storage oscilloscope (DSO-X-4104A, Keysight Technologies, USA). The same experiments were also repeated on a plain aluminium rod without baffles for comparison. The A-scans obtained from the experiments were further analysed by obtaining the frequency spectrum (see below).

III. RESULTS AND DISCUSSION

A. GMR FOR UP-CONVERSION OF L(0,2) TO L(0,3) MODE

1) 2D FFT ANALYSIS OF SIMULATION DATA ALONG THE AXIS

From the numerical analysis discussed in Section II-B, time-domain signals were collected along the axis at different points before the baffles and beyond the baffles along the

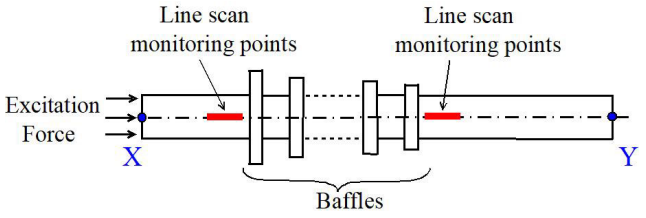

FIGURE 5. Schematic of the simulation set-up for data acquisition for 2D FFT analysis.

direction of wave propagation as in Fig. 5. A similar exercise of signal extraction was done from the same points in the bare rod also. 2D Fast Fourier Transform (2D FFT) analysis was done for signals obtained from both the cases and the plots were overlaid on the frequency-wavenumber ($f - k$) dispersion curves for a bare rod of 10mm diameter obtained from DISPERSE [60] software as shown in Fig. 6 (a)-(d). Note that the negative wavenumber corresponds to the modes present in the reflected waves observed at those points.

Fig. 6(a) refers to the 2D FFT plot obtained from data monitored at points at the incident side 'X' as in Fig. 5. Both L(0,2) and L(0,3) modes pass through the monitoring points without any reflections in this case. In Fig. 6(b), the monitoring points are moved after the baffle section and we can see that the L(0,2) mode is reflected from the other end 'Y' (in Fig.5). Whereas, in the case of GMR in Fig. 6(c) the monitoring points are before the baffles at the incident side 'X'. Both L(0,2) and L(0,3) modes pass through the monitoring points and a small amount of reflections of both the modes from the baffles can be observed. And in Fig. 6(d) the monitoring points are beyond the baffles. Any remaining L(0,2) mode passing through the baffles are converted to L(0,3) mode and we cannot see the reflection L(0,3) mode since it is a slow mode compared to L(0,2). These results clearly show the up-conversion of L(0,2) mode to L(0,3) mode at the centre frequency 0.5 MHz.

2) STFT OF SIMULATION AND EXPERIMENTAL DATA

The time-domain signals obtained from the numerical simulations in Section II-B were further analysed by plotting the time-frequency spectrogram (See Fig.7 (a) and (b)) obtained by applying the Short-Time Fourier Transformation (STFT, see [62] and [63] and citations therein for more details on this technique). The group velocity dispersion curves (see Fig. 2) obtained from DISPERSE [60] were converted to time-frequency dispersion curves and then overlaid on the spectrogram, as shown in Fig. 7(a). The dark spot in the spectrogram indicates the presence of only L(0,3) mode. A similar analysis was performed for a bare rod (without the baffles), and the results are shown in Fig. 7(b). We can observe in Fig. 7(b) that L(0,1), L(0,2) and L(0,3) modes exist in this case. The absence of L(0,2) mode in Fig. 7(a) clearly shows the up-conversion of L(0,2) mode to L(0,3) mode. A similar exercise was carried out on the experimental results obtained in Section II-C. The results in Fig. 8(a) and (b)

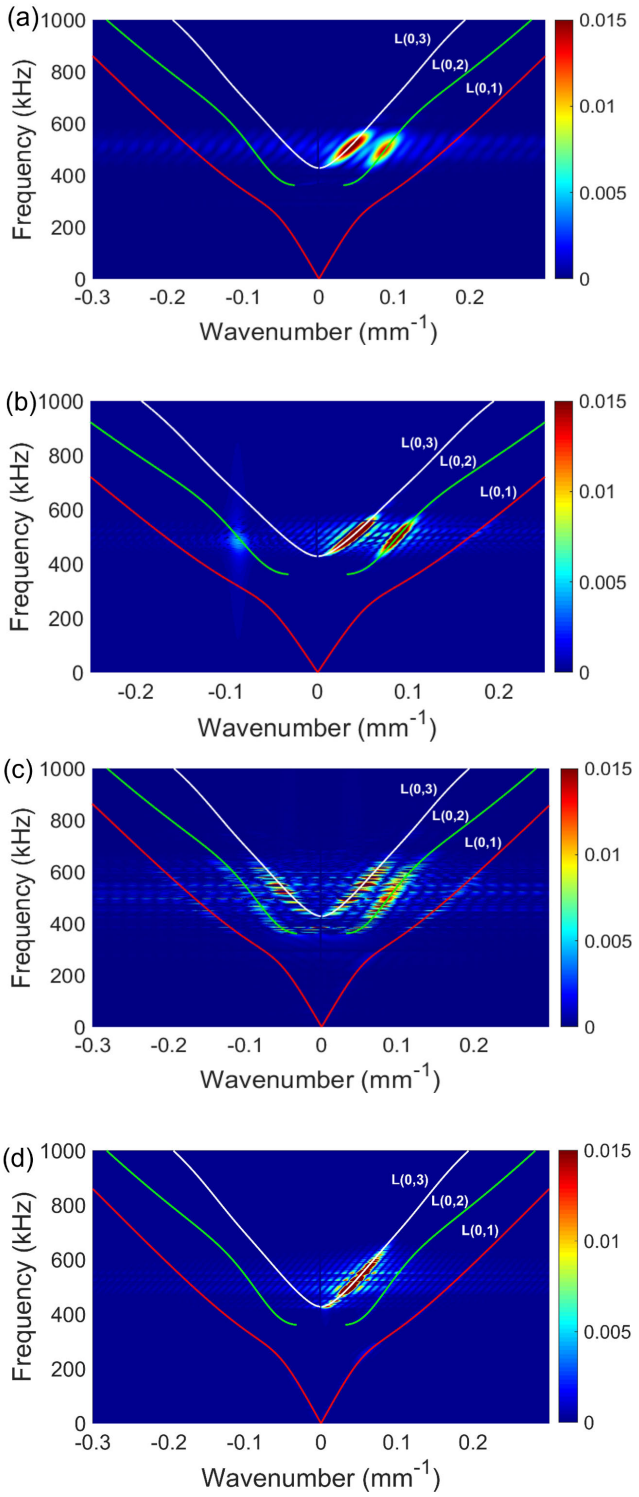

FIGURE 6. **Frequency-wavenumber dispersion plot of bare rod of 10mm diameter overlaid on 2D FFT plot of without GMR and with GMR cases. Without GMR (a) before baffle, (b) beyond baffle; with GMR (c) before baffle, (d) beyond baffle, clearly showing the up-conversion of L(0,2) mode to L(0,3) mode in presence of GMR at 0.5 MHz.**

corroborate the mode conversion phenomena observed in simulation results.

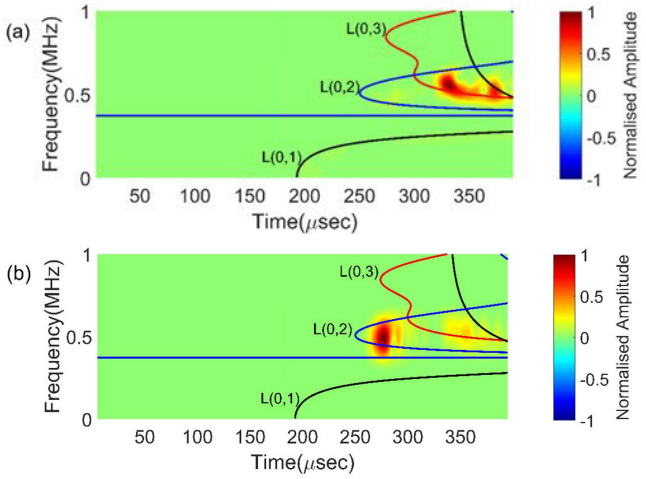

FIGURE 7. **Time spectrogram plot obtained from simulation (a) with GMR, (b) without GMR.**

B. DISCUSSION

The up-conversion of L(0,2) mode to L(0,3) mode at 0.5 MHz, achieved using the proposed GMR concept, is studied analytically in this section. Firstly, the group delay frequency spectrum of longitudinal wave modes L(0,n) in the GMR is calculated in Section III-B.1. From the group delay, the frequency spectrum of the group velocity for each mode is arrived at in Section III-B.2. The procedure to derive the frequency-wavenumber relation for the GMR is discussed further in the same section. Finally, the mode conversion is explicitly shown to arise from the physics behind the above relation.

1) GROUP DELAY CALCULATION

The dispersion relation for longitudinal waves in circular rods of radius 'a' is given by Pochhammer frequency equation [64],

$$\frac{2p}{a}(q^2+k^2)J_1(pa)J_1(qa)-(q^2-k^2)^2J_0(pa)J_1(qa) - 4k^2pqJ_1(pa)J_0(qa)=0, \qquad (1)$$

where $J_m(.)$ is the Bessel function of the first kind of order m; $p=\sqrt{\frac{\omega^2}{c_L^2}-k^2}$, $q=\sqrt{\frac{\omega^2}{c_T^2}-k^2}$; c_L and c_T are dilatational longitudinal bulk wave velocity and shear bulk wave velocity, respectively.

The roots of (1) provide the frequency spectrum for longitudinal waves in circular rod-type waveguides. It is used for deriving the frequency-dependent phase velocity and group velocity of all the modes in the family of longitudinal guided wave modes. However, the dispersion relation for the GMR introduced in this paper is not known. Hence, we may need to utilize the concept of group delay to identify the dispersion relation for complex shaped, anisotropic waveguides. Group delay is the time of travel for a wave propagating along a waveguide of diameter (D) for a given frequency (f), and this concept can be used in anisotropic

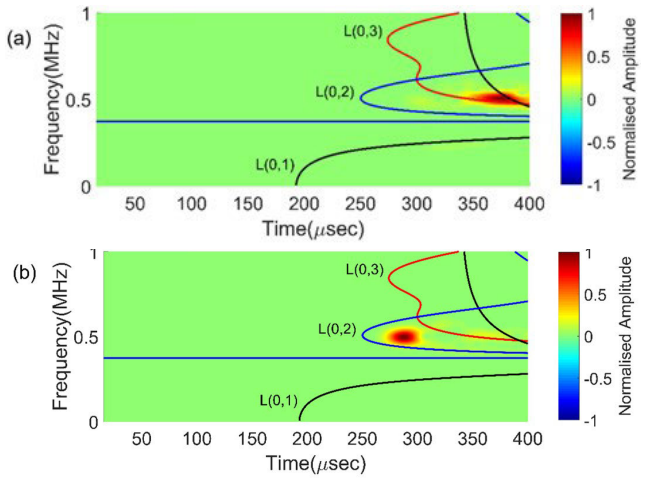

FIGURE 8. **Time spectrogram plot obtained from experiment (a) with GMR, (b) without GMR.**

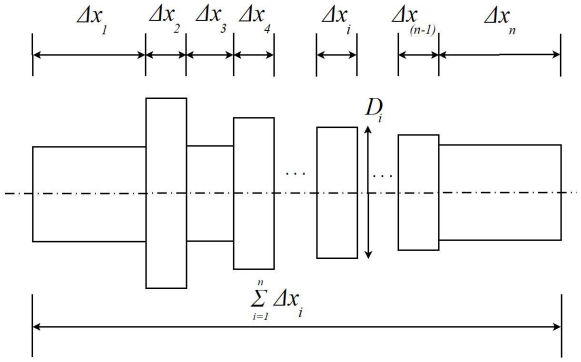

FIGURE 9. **Illustration of waveguide for group delay calculation.**

waveguides with a varying thickness within the same family of waves.

The group delay of the waveguide with a varying cross-section (as shown, for example, in Fig. 9 above) is given by [65],

$$GD(f) = \Sigma_{i=1}^{n} \frac{\Delta x_i}{C_g(D_i, f)} \tag{2}$$

where $C_g(D_i, f) = \frac{d\omega}{dk}$ is the group velocity of a waveguide of diameter D_i for frequency f. $C_g(D_i, f)$ is calculated from the Pochhammer frequency equation in (1) for different modes of axisymmetric longitudinal waves L(0,m), $m = 0,1,2$, etc.

Using (2), group delays of a waveguide of varying cross-section discussed in this paper are calculated for the L(0,1), L(0,2), and L(0,3) modes, and the results are shown in Fig. 10 below.

2) DISPERSION CALCULATION

From group delay, the group velocity of each mode at different frequencies is calculated by dividing the total length of the waveguide by group delay.

$$C_g^{L(0,m)}(f) = \frac{Length}{GD^{L(0,m)}(f)}, \tag{3}$$

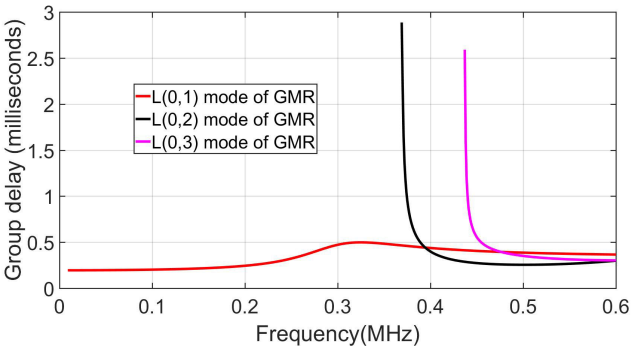

FIGURE 10. **Group delay as a function of frequency for the proposed GMR discussed in this paper.**

where $C_g^{L(0,m)}(f)$ is the group velocity of the waveguide for the longitudinal mode $L(0, m)$ at frequency f; $GD^{L(0,m)}(f)$ is the corresponding group delay.

Our objective is to find the frequency-dependent phase velocity relation so as to check any mode conversion occurring within the frequency band of interest. Prior work reports the indication of mode conversion when an equality of wavenumber may occur at a given frequency. For ex: Meeker et al. [66] predicted that a guided wave motion in one mode becomes extremely susceptible to coupling to another mode at frequencies where the two modes have equal phase velocities. Morvan et al. [67] argued that propagation of Lamb waves in a plate with an engraved periodic grating results in conversion to other modes. Each intersection of the curves, corresponding to wavevector versus frequency of the converted wave, with a Lamb wave dispersion curve indicates a possible conversion of the incident wave. Puthillath et al. [68] studied the energy transfer and mode conversion of ultrasonic guided wave propagation across waveguide transitions (say waveguide 'A' to waveguide 'B'). They observed that wherever the phase velocity dispersion curves overlap, the incident mode in waveguide 'A' will get mode converted to the overlapped mode in waveguide 'B', resulting in strong energy transfer across the transition. Along the same lines, here we seek to derive the expression for phase velocity for different longitudinal modes from (3) to check the possibility of mode conversions.

$C_g^{L(0,m)}(f)$ corresponding to all values of m are inversed to find $\frac{dk}{d\omega}$, and polynomial fitting is done in terms of variable frequency f.

$$\frac{dk^{L(0,m)}}{d\omega} = \Sigma_{n=0}^{N} a_n f^n. \tag{4}$$

The truncation of the series is suitably done for minimum error for each mode.

Integrating (4) with respect to f,

$$k^{L(0,m)} = 2\pi \Sigma_{n=0}^{N} a_n \frac{f^{n+1}}{n+1} + C, \tag{5}$$

where the constant C is determined from the limiting value of $C_g^{L(0,m)}(f)$ as follows. The generalised group velocity (C_g)

and phase velocity (C_p) relation is,

$$\frac{1}{C_g} = \frac{1}{C_p} - \frac{\omega}{C_p^2}\frac{dC_p}{d\omega}. \tag{6}$$

From the dispersion curve of normal cylindrical rods, when ω takes higher values $\frac{dC_p}{d\omega} \rightarrow 0$ as C_p converges to a constant value. This approximation is valid on the basis of many reported literatures [69], [70].

For limiting value of $\omega \rightarrow \infty$, $C_g \approx Cp$. Then,

$$\frac{dk^{L(0,m)}}{d\omega} \approx \frac{k}{\omega} \tag{7}$$

$$k^{L(0,m)} \approx \omega \frac{dk^{L(0,m)}}{d\omega} \tag{8}$$

Comparing (5) and (8),

$$C = f\frac{dk^{L(0,m)}}{df} - 2\pi\,\Sigma_{n=0}^{N} a_n \frac{f^{n+1}}{n+1}, \text{ as } \omega \rightarrow \infty \tag{9}$$

The constant, C, is found from (9) for modes L(0,1), L(0,2) and L(0,3). Using (5) and (9), the dispersion relation is obtained for all three modes, as shown in Fig. 11 below.

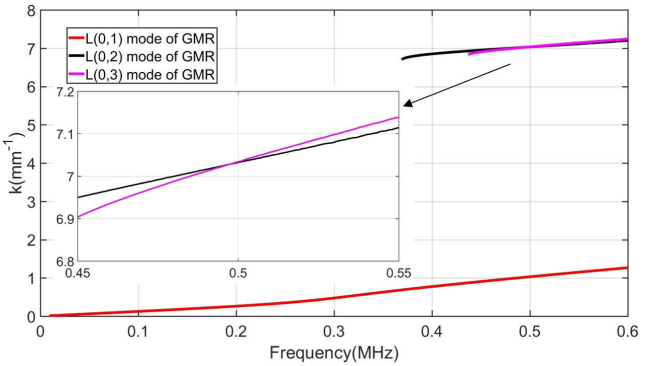

FIGURE 11. Dispersion of tapered waveguide showing L(0,1), L(0,2) and L(0,3) modes. Inset view shows the detailing of up-conversion of L(0,2) to L(0,3) mode at 0.5MHz.

We can observe that whenever the phase velocities in the pair of modes considered are the same, mode conversion can occur [66], [67], [68]. In this case, the phase velocities of L(0,2) and L(0,3) are the same at 0.5 MHz in Fig.11, indicating the conversion of L(0,2) mode to L(0,3) mode at this frequency. This model helped the authors optimize the parameters of the GMR, leading to the successful demonstration through experiments as discussed above.

IV. CONCLUSION

This paper demonstrates the novel application of graded metamaterial rods (or GMR) for up-conversion of modes within the longitudinal family of guided ultrasonic rod waves, best suited for optimal transduction of bulk ultrasonic waves in the specimen sample for sensing/ measurement applications. Finite element simulations and experimentation followed by analytical modelling elucidate the mode conversion of L(0,2) to L(0,3) for novel applications of such waveguide metamaterials in practical NDE applications such as transduction and remote measurement of material and environmental properties. Our analytical model can also be used as a framework for quick understanding of mode conversions in cylindrical rods of any diameters without recourse to laborious numerical analysis. Further work at our Laboratory is focused on the study of similar waveguide metamaterials tunable for any mode conversion of ultrasonic waves in selective applications.

REFERENCES

[1] L. C. Lynnworth, R. Cohen, J. L. Rose, J. O. Kim, and E. R. Furlong, "Vortex shedder fluid flow sensor," *IEEE Sensors J.*, vol. 6, no. 6, pp. 1488–1496, Dec. 2006, doi: 10.1109/JSEN.2006.883856.

[2] A. Gueddida et al., "Tubular phononic crystal sensor," *J. Appl. Phys.*, vol. 130, no. 10, Sep. 2021, Art. no. 105103, doi: 10.1063/5.0051660.

[3] S. Periyannan, P. Rajagopal, and K. Balasubramaniam, "Re-configurable multi-level temperature sensing by ultrasonic 'spring-like' helical waveguide," *J. Appl. Phys.*, vol. 119, no. 14, Apr. 2016, Art. no. 144502, doi: 10.1063/1.4945322.

[4] F. B. Cegla, P. Cawley, and M. J. S. Lowe, "Material property measurement using the quasi-Scholte mode—A waveguide sensor," *J. Acoust. Soc. Amer.*, vol. 117, no. 3, pp. 1098–1107, Mar. 2005, doi: 10.1121/1.1841631.

[5] R. Lucklum and N. Mukhin, "Enhanced sensitivity of resonant liquid sensors by phononic crystals," *J. Appl. Phys.*, vol. 130, no. 2, Jul. 2021, Art. no. 024508, doi: 10.1063/5.0046847.

[6] M. Laws, S. N. Ramadas, L. C. Lynnworth, and S. Dixon, "Parallel strip waveguide for ultrasonic flow measurement in harsh environments," *IEEE Trans. Ultrason., Ferroelectr., Freq. Control*, vol. 62, no. 4, pp. 697–708, Apr. 2015, doi: 10.1109/TUFFC.2014.006933.

[7] F. Ciampa, A. Mankar, and A. Marini, "Phononic crystal waveguide transducers for nonlinear elastic wave sensing," *Sci. Rep.*, vol. 7, no. 1, pp. 1–8, Nov. 2017, doi: 10.1038/s41598-017-14594-4.

[8] M. Miniaci and R. K. Pal, "Design of topological elastic waveguides," *J. Appl. Phys.*, vol. 130, no. 14, Oct. 2021, Art. no. 141101, doi: 10.1063/5.0057288.

[9] K. Arunachalam, V. R. Melapudi, L. Udpa, and S. S. Udpa, "Microwave NDT of cement-based materials using far-field reflection coefficients," *NDT E Int.*, vol. 39, no. 7, pp. 585–593, Oct. 2006, doi: 10.1016/j.ndteint.2006.03.001.

[10] J. L. Borgerson and H. Reis, "Torsional waveguide sensor system for monitoring the setting and hardening of concrete," *Insight Non-Destructive Test. Condition Monitor.*, vol. 49, no. 11, pp. 657–659, Nov. 2007, doi: 10.1784/insi.2007.49.11.657.

[11] V. Utsi and E. Utsi, "Measurement of reinforcement bar depths and diameters in concrete," in *Proc. 10th Int. Conf. Grounds Penetrating Radar*, Delft, The Netherlands, 2004, pp. 659–662.

[12] H. Shah, K. Balasubramaniam, and P. Rajagopal, "In-situ process- and online structural health-monitoring of composites using embedded acoustic waveguide sensors," *J. Phys. Commun.*, vol. 1, no. 5, Dec. 2017, Art. no. 055004, doi: 10.1088/2399-6528/aa8bfa.

[13] F. B. Cegla, P. Cawley, J. Allin, and J. Davies, "High-temperature (>500°c) wall thickness monitoring using dry-coupled ultrasonic waveguide transducers," *IEEE Trans. Ultrason., Ferroelectr., Freq. Control*, vol. 58, no. 1, pp. 156–167, Jan. 2011, doi: 10.1109/TUFFC.2011.1782.

[14] C.-K. Jen, J.-G. Legoux, and L. Parent, "Experimental evaluation of clad metallic buffer rods for high temperature ultrasonic measurements," *NDT E Int.*, vol. 33, no. 3, pp. 145–153, 2000, doi: 10.1016/S0963-8695(99)00042-0.

[15] S. Periyannan and K. Balasubramaniam, "Multi-level temperature measurements using ultrasonic waveguides," *Measurement*, vol. 61, pp. 185–191, Feb. 2015, doi: 10.1016/j.measurement.2014.10.050.

[16] S. Periyannan, P. Rajagopal, and K. Balasubramaniam, "Multiple temperature sensors embedded in an ultrasonic 'spiral-like' waveguide," *AIP Adv.*, vol. 7, no. 3, Mar. 2017, Art. no. 035201, doi: 10.1063/1.4977965.

[17] Z. Wang, J. Liu, C. Fang, K. Wang, L. Wang, and Z. Wu, "Nondestructive measurements of elastic constants of thin rods based on guided waves," *Mech. Syst. Signal Process.*, vol. 170, May 2022, Art. no. 108842, doi: 10.1016/j.ymssp.2022.108842.

[18] J. Wu, Y. Wang, W. Zhang, Z. Nie, R. Lin, and H. Ma, "Defect detection of pipes using Lyapunov dimension of duffing oscillator based on ultrasonic guided waves," *Mech. Syst. Signal Process.*, vol. 82, pp. 130–147, Jan. 2017, doi: 10.1016/j.ymssp.2016.05.012.

[19] X. Yu, P. Zuo, J. Xiao, and Z. Fan, "Detection of damage in welded joints using high order feature guided ultrasonic waves," *Mech. Syst. Signal Process.*, vol. 126, pp. 176–192, Jul. 2019, doi: 10.1016/j.ymssp.2019.02.026.

[20] S. Majhi, A. Mukherjee, N. V. George, V. Karaganov, and B. Uy, "Corrosion monitoring in steel bars using laser ultrasonic guided waves and advanced signal processing," *Mech. Syst. Signal Process.*, vol. 149, Feb. 2021, Art. no. 107176, doi: 10.1016/j.ymssp.2020.107176.

[21] S. K. Sikundalapuram Ramesh, M. C. Thippeswamy, P. Rajagopal, and K. Balasubramaniam, "Elastic metamaterial rod for mode filtering in ultrasonic applications," *Electron. Lett.*, vol. 56, no. 19, pp. 1024–1027, Sep. 2020, doi: 10.1049/el.2020.1576.

[22] M. C. Thippeswamy, S. A. R. Kuchibhatla, and P. Rajagopal, "Concentric shell gradient index metamaterials for focusing ultrasound in bulk media," *Ultrasonics*, vol. 114, Jul. 2021, Art. no. 106424, doi: 10.1016/j.ultras.2021.106424.

[23] J. B. Pendry, D. Schurig, and D. R. Smith, "Controlling electromagnetic fields," *Science*, vol. 312, no. 5781, pp. 1780–1782, Jun. 2006, doi: 10.1126/science.1125907.

[24] K. K. Amireddy, K. Balasubramaniam, and P. Rajagopal, "Holey-structured metamaterial lens for subwavelength resolution in ultrasonic characterization of metallic components," *Appl. Phys. Lett.*, vol. 108, no. 22, Jun. 2016, Art. no. 224101, doi: 10.1063/1.4950967.

[25] J. Zhu et al., "A holey-structured metamaterial for acoustic deep-subwavelength imaging," *Nature Phys.*, vol. 7, no. 1, pp. 52–55, Nov. 2010, doi: 10.1038/nphys1804.

[26] K. K. Amireddy, K. Balasubramaniam, and P. Rajagopal, "Deep sub-wavelength ultrasonic imaging," in *Proc. AIP Conf.*, Provo, UT, USA, 2018, vol. 1949, no. 1, Art. no. 020025, doi: 10.1063/1.5031522.

[27] T. Chen, C. Wang, and D. Yu, "Pressure amplification and directional acoustic sensing based on a gradient metamaterial coupled with space-coiling structure," *Mech. Syst. Signal Process.*, vol. 181, Dec. 2022, Art. no. 5109499, doi: 10.1016/j.ymssp.2022.109499.

[28] H. Chen and C. T. Chan, "Acoustic cloaking in three dimensions using acoustic metamaterials," *Appl. Phys. Lett.*, vol. 91, no. 18, Oct. 2007, Art. no. 183518, doi: 10.1063/1.2803315.

[29] A. N. Norris, "Acoustic cloaking theory," *Proc. Roy. Soc. A, Math., Phys. Eng. Sci.*, vol. 464, no. 2097, pp. 2411–2434, Apr. 2008, doi: 10.1098/rspa.2008.0076.

[30] J. B. Pendry, "Negative refraction makes a perfect lens," *Phys. Rev. Lett.*, vol. 85, no. 18, pp. 3966–3969, Oct. 2000, doi: 10.1103/PhysRevLett.85.3966.

[31] J. B. Pendry, "Negative refraction," *Contemp. Phys.*, vol. 45, no. 3, pp. 191–202, May 2006, doi: 10.1080/00107510410001667434.

[32] K. P. Logakannan, V. Ramachandran, J. Rengaswamy, and D. Ruan, "Dynamic performance of a 3D re-entrant structure," *Mech. Mater.*, vol. 148, Sep. 2020, Art. no. 103503, doi: 10.1016/j.mechmat.2020.103503.

[33] X. Ren, J. Shen, P. Tran, T. D. Ngo, and Y. M. Xie, "Design and characterisation of a tuneable 3D buckling-induced auxetic metamaterial," *Mater. Design*, vol. 139, pp. 336–342, Feb. 2018, doi: 10.1016/j.matdes.2017.11.025.

[34] N. Gaspar, X. Ren, C. Smith, J. Grima, and K. Evans, "Novel honeycombs with auxetic behaviour," *Acta Mater.*, vol. 53, no. 8, pp. 2439–2445, May 2005, doi: 10.1016/j.actamat.2005.02.006.

[35] Q. Zhang et al., "A dynamic poroelastic model for auxetic polyurethane foams involving viscoelasticity and pneumatic damping effects in the linear regime," *Mech. Syst. Signal Process.*, vol. 179, Nov. 2022, Art. no. 109375, doi: 10.1016/j.ymssp.2022.109375.

[36] H. K. Maheshwari and P. Rajagopal, "Novel locally resonant and widely scalable seismic metamaterials for broadband mitigation of disturbances in the very low frequency range of 0–33 Hz," *Soil Dyn. Earthquake Eng.*, vol. 161, Oct. 2022, Art. no. 107409, doi: 10.1016/j.soildyn.2022.107409.

[37] Y. Jin et al., "Design of cylindrical honeycomb sandwich meta-structures for vibration suppression," *Mech. Syst. Signal Process.*, vol. 163, Jan. 2022, Art. no. 108075, doi: 10.1016/j.ymssp.2021.108075.

[38] E. D. Nobrega, F. Gautier, A. Pelat, and J. M. C. Dos Santos, "Vibration band gaps for elastic metamaterial rods using wave finite element method," *Mech. Syst. Signal Process.*, vol. 79, pp. 192–202, Oct. 2016, doi: 10.1016/j.ymssp.2016.02.059.

[39] Y. Bai, L. Gu, X. Wang, and Z. Huang, "Passive, remote and omnidirectional suppression of sound source radiation via an acoustic superscatterer," *J. Phys. D, Appl. Phys.*, vol. 55, no. 1, Oct. 2021, Art. no. 015302, doi: 10.1088/1361-6463/ac2692.

[40] V. P. Ramachandran and P. Rajagopal, "Bandwidth-limited passive suppression of cylindrical source radiation using metamaterial based acoustic superscatterers," *J. Sound Vibrat.*, vol. 560, Sep. 2023, Art. no. 117767, doi: 10.1016/j.jsv.2023.117767.

[41] J. M. De Ponti et al., "Experimental investigation of amplification, via a mechanical delay-line, in a rainbow-based metamaterial for energy harvesting," *Appl. Phys. Lett.*, vol. 117, no. 14, Oct. 2020, Art. no. 143902, doi: 10.1063/5.0023544.

[42] J. M. De Ponti, A. Colombi, R. Ardito, F. Braghin, A. Corigliano, and R. V. Craster, "Graded elastic metasurface for enhanced energy harvesting," *New J. Phys.*, vol. 22, no. 1, Jan. 2020, Art. no. 013013, doi: 10.1088/1367-2630/ab6062.

[43] S.-H. Jo, H. Yoon, Y. C. Shin, and B. D. Youn, "A graded phononic crystal with decoupled double defects for broadband energy localization," *Int. J. Mech. Sci.*, vol. 183, Oct. 2020, Art. no. 105833, doi: 10.1016/j.ijmecsci.2020.105833.

[44] J. M. De Ponti, L. Iorio, E. Riva, R. Ardito, F. Braghin, and A. Corigliano, "Selective mode conversion and rainbow trapping via graded elastic waveguides," *Phys. Rev. Appl.*, vol. 16, no. 3, Sep. 2021, Art. no. 034028, doi: 10.1103/PhysRevApplied.16.034028.

[45] H.-W. Dong et al., "Reflective metasurfaces with multiple elastic mode conversions for broadband underwater sound absorption," *Phys. Rev. Appl.*, vol. 17, no. 4, Apr. 2022, Art. no. 044013, doi: 10.1103/PhysRevApplied.17.044013.

[46] Y. Tian, Y. Song, Y. Shen, and Z. Yu, "A metamaterial ultrasound mode convertor for complete transformation of Lamb waves into shear horizontal waves," *Ultrasonics*, vol. 119, Feb. 2022, Art. no. 106627, doi: 10.1016/j.ultras.2021.106627.

[47] Y. Tian, Y. Shen, X. Qin, and Z. Yu, "Enabling the complete mode conversion of Lamb waves into shear horizontal waves via a resonance-based elastic metamaterial," *Appl. Phys. Lett.*, vol. 118, no. 1, Jan. 2021, Art. no. 014101, doi: 10.1063/5.0032802.

[48] J. M. De Ponti, L. Iorio, and R. Ardito, "Graded elastic meta-waveguides for rainbow reflection, trapping and mode conversion," *EPJ Appl. Metamater.*, vol. 9, no. 6, p. 5, Feb. 2022, doi: 10.1051/epjam/2022004.

[49] A. Colombi, P. Roux, S. Guenneau, P. Gueguen, and R. V. Craster, "Forests as a natural seismic metamaterial: Rayleigh wave bandgaps induced by local resonances," *Sci. Rep.*, vol. 6, no. 1, pp. 1–7, Jan. 2016, doi: 10.1038/srep19238.

[50] A. Colombi et al., "Enhanced sensing and conversion of ultrasonic Rayleigh waves by elastic metasurfaces," *Sci. Rep.*, vol. 7, no. 1, p. 6750, Jul. 2017, doi: 10.1038/s41598-017-07151-6.

[51] Z. Tian and L. Yu, "Rainbow trapping of ultrasonic guided waves in chirped phononic crystal plates," *Sci. Rep.*, vol. 7, no. 1, Jan. 2017, Art. no. 40004, doi: 10.1038/srep40004.

[52] K. K. Amireddy, K. Balasubramaniam, and P. Rajagopal, "Deep subwavelength ultrasonic imaging using optimized holey structured metamaterials," *Sci. Rep.*, vol. 7, no. 1, Aug. 2017, Art. no. 7777, doi: 10.1038/s41598-017-08036-4.

[53] K. K. Amireddy, K. Balasubramaniam, and P. Rajagopal, "Porous metamaterials for deep sub-wavelength ultrasonic imaging," *Appl. Phys. Lett.*, vol. 113, Sep. 2018, Art. no. 124102, doi: 10.1063/1.5045087.

[54] S. R. S. Kumar, V. K. Krishnadas, K. Balasubramaniam, and P. Rajagopal, "Higher harmonics suppression using nonlinear waveguide metamaterial rod," in *Review of Progress in Quantitative Nondestructive Evaluation*, 2019.

[55] C. T. Manjunath and P. Rajagopal, "Lensing in the ultrasonic domain using negative refraction induced by material contrast," *Sci. Rep.*, vol. 9, no. 1, Apr. 2019, Art. no. 6368, doi: 10.1038/s41598-019-42655-3.

[56] V. K. Krishnadas, K. Balasubramaniam, and P. Rajagopal, "Higher harmonics suppression using nonlinear waveguide metamaterial rod," in Proc. 46th Annu. Rev. Prog. Quant. Nondestruct. Eval. 2019, Paper QNDE2019-6943.

[57] S. R. S. Kumar, V. K. Krishnadas, K. Balasubramaniam, and P. Rajagopal, "Waveguide metamaterial rod as mechanical acoustic filter for enhancing nonlinear ultrasonic detection," *APL Mater.*, vol. 9, no. 6, p. 061115, Jun. 2021, doi: 10.1063/5.0051412.

[58] M. Bavencoffe, A.-C. Hladky-Hennion, B. Morvan, and J.-L. Izbicki, "Attenuation of Lamb waves in the vicinity of a forbidden band in a phononic crystal," *IEEE Trans. Ultrason., Ferroelectr., Freq. Control*, vol. 56, no. 9, pp. 1960–1967, Sep. 2009, doi: 10.1109/TUFFC.2009.1272.

[59] A. A. Jacob, P. Rajagopal, and K. Balasubramaniam, "Selective modal excitation for optimization of waveguide based bulk ultrasonic transducers," *NDT E Int.*, vol. 94, pp. 47–55, Mar. 2018, doi: 10.1016/j.ndteint.2017.11.005.
[60] B. Pavlakovic, M. Lowe, D. Alleyne, and P. Cawley, "Disperse: A general purpose program for creating dispersion curves," in *Review of Progress in Quantitative Nondestructive Evaluation*, vol. 16, D. O. Thompson and D. E. Chimenti, Eds. Boston, MA, USA: Springer, 1997, pp. 185–192, doi: 10.1007/978-1-4615-5947-4_24.
[61] *ABAQUS/Standard User's Manual (Version 6.12)*, Dassault Systèmes, Providence, RI, USA, 2014.
[62] K. Xu, D. Ta, and W. Wang, "Multiridge-based analysis for separating individual modes from multimodal guided wave signals in long bones," *IEEE Trans. Ultrason., Ferroelectr., Freq. Control*, vol. 57, no. 11, pp. 2480–2490, Nov. 2010, doi: 10.1109/TUFFC.2010.1714.
[63] P. Ray, B. Srinivasan, K. Balasubramaniam, and P. Rajagopal, "Monitoring pipe wall integrity using fiber Bragg grating-based sensing of low-frequency guided ultrasonic waves," *Ultrasonics*, vol. 90, pp. 120–124, Nov. 2018, doi: 10.1016/j.ultras.2018.06.009.
[64] J. Achenbach, *Wave Propagation in Elastic Solids*, 1st ed. Amsterdam, The Netherlands: Elsevier, 1973.
[65] L. De Marchi, A. Marzani, N. Speciale, and E. Viola, "Prediction of pulse dispersion in tapered waveguides," *NDT E Int.*, vol. 43, no. 3, pp. 265–271, Apr. 2010, doi: 10.1016/j.ndteint.2009.12.004.
[66] T. R. Meeker and A. H. Meitzler, "2—Guided wave propagation in elongated cylinders and plates," in *Physical Acoustics*, W. P. Mason, Ed. New York, NY, USA: Academic, 1964, pp. 111–167. [Online]. Available: https://www.sciencedirect.com/science/article/pii/B9781483228570500083, doi: 10.1016/B978-1-4832-2857-0.50008-3.
[67] B. Morvan, A.-C. Hladky-Hennion, D. Leduc, and J.-L. Izbicki, "Ultrasonic guided waves on a periodical grating: Coupled modes in the first Brillouin zone," *J. Appl. Phys.*, vol. 101, no. 11, Jun. 2007, Art. no. 114906, doi: 10.1063/1.2737348.
[68] P. Puthillath, J. M. Galan, B. Ren, C. J. Lissenden, and J. L. Rose, "Ultrasonic guided wave propagation across waveguide transitions: Energy transfer and mode conversion," *J. Acoust. Soc. Amer.*, vol. 133, no. 5, pp. 2624–2633, May 2013, doi: 10.1121/1.4795805.
[69] A. Ghavamian, F. Mustapha, B. T. Baharudin, and N. Yidris, "Detection, localisation and assessment of defects in pipes using guided wave techniques: A review," *Sensors*, vol. 18, no. 12, p. 4470, Dec. 2018, doi: 10.3390/s18124470.
[70] C. J. Lissenden, "Nonlinear ultrasonic guided waves—Principles for nondestructive evaluation," *J. Appl. Phys.*, vol. 129, no. 2, Jan. 2021, Art. no. 021101, doi: 10.1063/5.0038340.

S. R. SANDEEP KUMAR received the bachelor's degree in mechanical engineering from the Vasavi College of Engineering, Hyderabad, Telangana, India, in 2009. He is currently pursuing the dual M.S. and Ph.D. degree with the Indian Institute of Technology Madras (IIT Madras), Chennai, Tamil Nadu, India. He conducts his research at the Centre for Nondestructive Evaluation (CNDE), IIT Madras. His research interests include ultrasonic NDE and waveguide metamaterials.

VINEETH P. RAMACHANDRAN received the B.Tech. degree in mechanical engineering from the Visvesvaraya National Institute of Technology, Nagpur, MH, India, in 2008. He is currently pursuing the Ph.D. degree in mechanical engineering with the Indian Institute of Technology Madras (IIT Madras), Chennai, India. From 2008 to 2019, he was a Scientist with the Naval Physical and Oceanographic Laboratory, Kochi, Kerala, India. Since 2019, he has been with the DRDO Young Scientists' Laboratory for Smart Materials, Hyderabad, India. His research interests include design and development of underwater transducers and acoustic metamaterials. He is a Life Member of the Acoustical Society of India and the Institute of Smart Structures and Systems.

KRISHNAN BALASUBRAMANIAM received the bachelor's degree in mechanical engineering from the Regional Engineering College, University of Madras, Tiruchirappalli, India, in 1984, and the M.S. and Ph.D. degrees from Drexel University, Philadelphia, PA, USA, in 1986 and 1989, respectively. He is currently the Institute and Chair Professor with the Department of Mechanical Engineering and the Head of the Centre for Nondestructive Evaluation, Indian Institute of Technology Madras (IIT Madras), which he founded in 2001. Before joining IIT Madras in 2000, he was employed at Mississippi State University. His research interests include non-destructive evaluation with applications in the fields of maintenance, quality assurance, manufacturing, and design.

PRABHU RAJAGOPAL received the B.Tech. and M.Tech. (D.D.) degrees from the Indian Institute of Technology Madras (IIT Madras) and the Ph.D. and Post-Doctoral degrees from Imperial College London. He has expertise in remote Nondestructive Evaluation and Structural Health Monitoring, focusing on waveguide ultrasonic, robotics, and management of large scale inspection datasets. His work on metamaterials is expanding, with exciting applications for seismic and vibration damping and non-linear ultrasonics. He also helps companies improve sensor performance using simulation, analysis, and analytics. With over 25 funded projects, 225 technical articles, 45 filings, and 21 granted IPs, he is widely recognized for work on remote asset management in the marine, energy and mobility sectors, and a social focus on water, health, and sanitation.